Proc. Nat. Acad. Sci. USA
Vol. 71, No. 11, pp. 4298–4302, November 1974

The Three-Dimensional Structure of a Phosphorylcholine-Binding Mouse Immunoglobulin Fab and the Nature of the Antigen Binding Site

(x-ray diffraction/domain structure/hypervariable cavity/hapten binding/antibody diversity)

DAVID M. SEGAL*†, EDUARDO A. PADLAN*, GERSON H. COHEN*, STUART RUDIKOFF‡, MICHAEL POTTER‡, AND DAVID R. DAVIES*

* Laboratory of Molecular Biology, NIAMDD; † Immunology Branch, NCI; ‡ Laboratory of Cell Biology, NCI; National Institutes of Health, Bethesda, Maryland 20014

Communicated by Elvin A. Kabat, August 12, 1974

ABSTRACT **The structure of the Fab of McPC 603, a mouse myeloma protein with phosphorylcholine binding activity, has been determined to 3.1-Å resolution. The four domains are found to be structurally similar with a well-defined double-layer structure. A large cavity exists at one end of the fragment, the walls of which are formed exclusively of hypervariable residues. Phosphorylcholine binds in this cavity and forms specific interactions with several well-defined amino-acid side chains of the protein. The hapten is bound asymmetrically and interacts more with the heavy chain than with the light chain.**

We have been investigating the nature of antibody–antigen interactions by means of a crystallographic investigation of the Fab fragments of mouse myeloma proteins with known binding specificity (1, 2). The testing of myeloma proteins in mice for antigen-binding activity has revealed that many of them interact by precipitation, agglutination, or complement-fixation with common natural antigens from the environment of the mouse (3, 4). Immunochemical analysis of myeloma protein–antigen interactions has in many cases led to the identification of the chemical group (hapten) on the antigen molecule.

Antibodies, induced to dextran, levan, and phosphorylcholine in mice, share cross-specific antigenic (idiotypic) determinants with myeloma proteins of corresponding specificity (5, 6; M. Potter and R. Lieberman, unpublished observations). These findings strongly suggest the close relationship of antigen-binding myeloma proteins in mice to natural or induced antibodies. One of these myeloma proteins, from McPC 603, precipitates with antigens from several pathogenic organisms, and has been demonstrated to bind specifically to phosphorylcholine (3). We have previously reported crystallization of the Fab fragment of McPC 603 protein (1) and its structure at 4.5-Å resolution together with the location of its phosphorylcholine-binding site (2). Here we present the results of a 3.1-Å structure determination and the molecular details of phosphorylcholine binding. We compare these results with the crystallographic results on a human Fab fragment with hydroxyvitamin K_1 binding properties (7, 8), and with two human Bence-Jones proteins (9, 10).

MATERIALS AND METHODS

The preparation and crystallization of McPC 603 pepsin Fab has been described (1). The crystals used were obtained from 42% saturated ammonium sulfate solutions, 0.1 M imidazole (pH 7.0). They belong to the space group $P6_3$ with a = b = 162.5, c = 60.8 Å. Heavy atom derivatives were prepared by soaking the crystals in solutions containing $TmCl_3$, $K_2Pt(CNS)_6$, iodine, and combinations of these (E. A. Padlan, D. M. Segal, G. H. Cohen, T. Spande, and D. R. Davies, in preparation). Approximately 11,000 reflections (mean figure of merit 0.73) were used to calculate a 3.1-Å electron density map. Details of the crystallographic analysis are being published elsewhere. A Kendrew skeletal model of the entire Fab has been constructed with the aid of the amino-acid sequence, which is for the most part known. An optical comparator of the type proposed by Richards (11), but with the mirror parallel to the electron density sections, was used to facilitate the model building. Coordinates have been measured for the variable region of the molecule and improved by the Diamond model-building program (12). Hapten binding has been studied by difference-Fourier techniques using data from crystals of McPC 603 Fab soaked in saturating concentrations of phosphorylcholine as described (2), but here extended to 3.1-Å resolution.

The amino-acid sequence of the variable portion of the heavy chain (V_H) is completely known (Table 1). Approximately half the C_H1 region sequence has been determined (Rudikoff, unpublished), and a substantial part of the remainder may be surmised from its expected homology with MOPC 315 (13). The V_L sequence is mostly known and its determination is being actively pursued. The constant portion of the light chain (C_L) is assumed to be identical with the sequence of the C region of other murine K light chains (14, 15). Light chain hypervariable regions were assigned according to Wu and Kabat (16). In the heavy chain these regions were identified by comparison with other heavy chain sequences, with deletions and insertions introduced to maximize homology (17).

RESULTS

The electron density map is clear enough to permit tracing the course of the polypeptide chain with confidence. While many of the smaller side groups are lost in the background noise, particularly those on the exterior of the molecule, the larger aromatic side chains are for the most part clearly visible, and serve as markers in fitting the amino-acid sequence to the map. Although the four disulfide bridges were located, they do not exhibit the highest peak density in each domain.

Overall Structure. The overall appearance of the IgA(K) 603 Fab is very similar to that previously observed in the human

Abbreviations: C_H1 and V_H; C_L and V_L signify the constant and variable domains of the heavy (H) and light (L) chains, respectively, of the Fab. H1, H2, and H3; L1, L2, and L3 are the first, second, and third hypervariable regions of the H and L chains, respectively.

TABLE 1. *Variable region sequence of McPC 603**

	1 10 20 30 40 50 58a 58b
V_H:	E-V-K-L-V-E-S-G-G-G-L-V-Q-P-G-G-S-L-R-L-S-C-A-T-S-G-F-T-F-S-B-F-Y-M-E-W-V-R-Q-P-P-G-K-R-L-E-W-I-A-A-S-R-B-K-G-B-K-Y-T—T-
	60 70 80 90 100 a b 110
	Z-Y-S-A-S-V-K-G-R-F-I-V-S-R-B-T-S-Z-S-I-L-Y-L-Q-M-N-A-L-R-A-E-D-T-A-I-Y-Y-C-A-R-N-Y-Y-G-S-T-W-Y-F-D-V-W-G-A-G-T-T-V-T-V
	1 10 20 27 27a 27b 27c 27d 27e 27f 30 40
V_L‡:	D-I-V-M-T-Q-S-P-S-S-L-S-V-S-A-G-E-R-V-T-M-S-C-K-S-S-Z—S—L—L—B—S—G—B-Z-K-B-F-L-A-W-Y-Z-(Z)-K-P-G-Z-P-P-K-L-I-Y

* Heavy chain numbering is that previously reported (17), with gaps and insertions introduced to maximize homologies with other heavy chain sequences. Light chain numbering is according to Wu and Kabat (16).

‡ The first 35 residues of this light chain sequence have previously been reported (25).

IgG(λ) New Fab (7) and in the human Mcg Bence-Jones dimer (9). The fragment has the overall dimensions 40 × 50 × 75 Å. It consists of two globular regions, each approximately 40 × 40 × 50 Å. Each globular region in turn is made up of two homologous domains; V_H:V_L in the variable region, and C_H1:C_L in the constant region. These pairs of domains are related to one another by an approximate 2-fold axis of symmetry. The pseudo 2-fold axes from the two regions are not colinear, but make an angle of approximately 135°.

Domain Structure. In both V and C regions the basic domain structure consists of straight segments of polypeptide chain arranged in two layers and forming a sandwich-like structure. The chains in each layer have the frequently observed left-handed twist.

Fig. 1 is a schematic representation of the folding for the variable and constant domains. Adjacent segments within each layer are antiparallel to each other and frequently assume a β-pleated sheet configuration. The interior of the sandwich contains principally hydrophobic residues. The intradomain disulfide and the invariant tryptophan are in close proximity and are located approximately in the middle of the domain. The extended segments are linked by bends with varying degrees of sharpness. The electron density in many of the tight bends can be fitted with β-bend configurations (18).

We have adopted the numbering scheme shown in Fig. 1, where we have denoted the stretches as S1, S2, S3, . . . S9 and bends as B12, B23, B34, . . . B89 with the bend numbers representing the stretches connected. Thus, we can think of the variable domains as consisting of nine stretches with eight bends and the constant domains as having seven stretches with six bends. Segments S4 and S5 and bend B45 are missing in the constant domains; this additional loop in the variable domains contains the second hypervariable regions of the light and heavy chains. Segments S1, S2, S6, and S7 form one layer of the sandwich and segments S3, S8, and S9 form the other. In the variable domains the additional loop occurs at the edge of the sandwich and is located approximately in the three-segment layer. The extended segments in the constant domains, are on the average, slightly longer than the homologous segments in the variable domains.

Quaternary Structure. It was clear even at low resolution that the two domains of each chain were oriented approximately at right angles to each other. In addition, the four domains of the fragment can be regarded as being located on the vertices of an elongated but distorted tetrahedron (2). The long axes of the domains of the light chain make an angle of approximately 100° with each other, while the corresponding angle for the heavy chain is approximately 80°. This results in a center to center distance of about 40 Å between the intra-domain disulfides of V_L and C_L compared with a distance of about 30 Å between V_H and C_H1. Similar results have also been observed in the human Fab New (7) and in the human Mcg Bence-Jones dimer (9). A possible explanation of this distortion of the symmetry of the McPC 603 fragment may lie in the more extensive interaction between the constant and variable domains of the heavy chain when compared with those of the light chain.

The close approach of the two heavy domains (V_H, C_H1) appears to be facilitated by the presence at the interface of amino acids with small side chains. For instance, involved in this contact are the stretch Gly-Gly-Gly (residues 8–10) in S1 and the stretch Gly-Ala-Gly (residues 109–111) in S9. In addi-

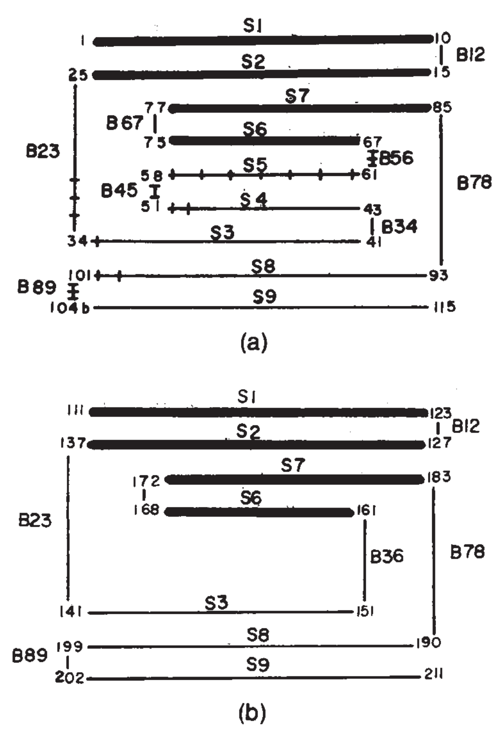

FIG. 1. (*a*) A schematic representation of the heavy chain variable domain. The relatively extended segments are denoted by S and are numbered sequentially from the NH_2 terminus. The bends B are numbered according to the segments they connect. The hypervariable regions (31–35, 49–66, 99–104b) are represented by the perpendicular bars. The segments drawn with thick lines belong to one layer of the sandwich structure, and the thin segments belong to the other layer. (*b*) A comparable schematic drawing of the C_L domain. Note the absence of the loop S4, B45, S5, which is only found in the variable domains.

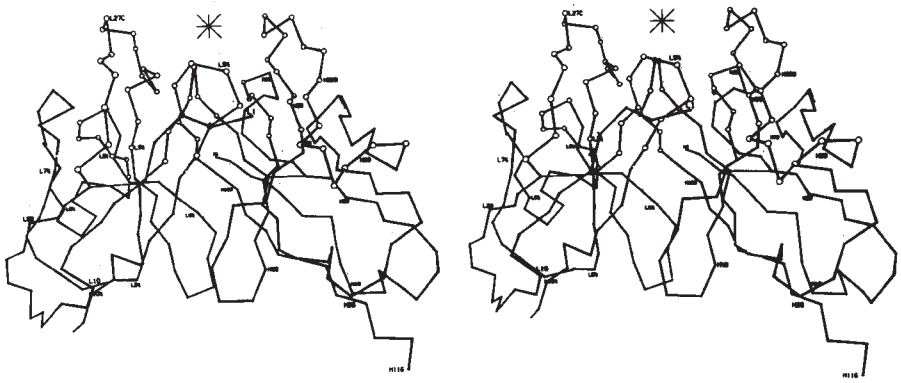

FIG. 2. Stereo drawing of the α-carbon skeleton of the variable region. Open lines represent the light chain and solid lines the heavy chain. The hypervariable residues are represented by the large open circles. The star marks the location of the large hypervariable cavity.

tion, this heavy chain interdomain interaction involves no charged amino-acid side chains.

It is apparent that the dominant force maintaining the structural integrity of the McPC 603 Fab is due to the strong lateral interactions between homologous domains (V_H–V_L; C_H1–C_L) rather than the much weaker longitudinal interactions between domains of the same chain. The interactions between the two constant domains occurs principally between the layers containing segments S1, S2, S7, and S6. The interaction between the variable domains is quite different, and involves the segments S3, S8, and S9, as well as a major portion of the extra loops S4-S5. Additional intervariable domain contacts occur between parts of the hypervariable loops, especially in the regions B23 of the L chain and B89 of the H chain.

The constant region is more compact than the variable region, probably as a result of having fewer bulky residues in the interface between C_L and C_H1. The interacting layers in this region are about 10 Å apart; this results in a distance between the two S-S bridges of 18 Å. In the absence of complete sequence information for C_H1, the interactions across the C region interface cannot be determined with confidence.

In the variable region the interacting segments are 12–15 Å apart, and this greater separation is reflected in the distance between the intervariable domain disulfides of approximately 25 Å. In spite of our lack of complete light chain sequence, many of the interdomain contact residues can be identified. They span the complete range of variability. Some, for example, Leu 45 and Trp 47, have been found in all heavy chain sequences, and Gln 39 has been found in most (17, 19). Similarly in the light chain, Tyr 36, which makes contact across the interface, is the residue most frequently found in this position in kappa chains (19). In addition, many of the interacting residues are found in the hypervariable regions. Indeed, the large loop produced by the six-residue insertion in L1 is in intimate contact with most of the residues in H3. Moreover, some residues in L3 interact with residues in both hypervariable and nonhypervariable portions of the V_H domain.

The Antigen-Binding Site. The 4.5-Å investigation revealed the location of the hapten-binding site (2). The appearance of two peaks on the difference electron density map led to the suggestion that, in the native crystals, the phosphate binding site was occupied by a sulfate ion. The present native electron density map at 3.1-Å resolution shows a large peak, tetrahedral in appearance, and making contact with side chains, in the phosphate position. The choline site is revealed by a 3.1-Å difference map between native and phosphorylcholine-soaked crystals.

The site of hapten binding is in a large wedge-shaped cavity, which exists at the amino-terminal end of the molecule (Fig. 2). The cavity is approximately 12 -Å deep, 15-Å wide at the mouth, and 20-Å long, the walls of which are lined exclusively with hypervariable residues (16). Only five of the hypervariable regions contribute to the formation of the cavity; these are the L1, L3, H1, H2, and H3. The portion homologous to the fourth hypervariable region (residues 82–89), reported in human heavy chains (20), occurs predominantly in the bend B78 at the COOH-terminal end of the variable region and is quite removed from the cavity. L2 likewise does not form a part of the walls of the cavity, being screened from it by the large loop containing L1. The insertions in L1, H2, and H3 cause these hypervariable loops to extend farther out, thus increasing the cavity depth.

The phosphorylcholine occupies only a small part of the cavity and is bound asymmetrically (Fig. 3), being closer to the H chain than to the L chain. The choline moiety is bound in the interior of the cavity with the phosphate group more towards the exterior. The phosphate group appears to be exclusively bound by the H chain; in particular, specific interactions are formed between the phosphate and Tyr 33(H) and Arg 52(H). The hydroxyl group of Tyr 33(H) is apparently hydrogen bonded to one of the oxygens of the phosphate, as is one of the amino groups of the arginine side chain. Moreover, the close proximity of the positively charged guanidinium group of Arg 52(H) to the negatively charged phosphate should produce a large favorable electrostatic interaction. There is also in the immediate vicinity of the phosphate another positive group, that of Lys 54(H), also of the heavy chain which could help neutralize the negative charge of this portion of the hapten. The choline group appears to interact with both the L and H chains. The acidic side chain of Glu 35(H) is about 5 Å away from the positively charged nitrogen of the choline. In addition, there are van der Waals interactions between the choline and main chain atoms

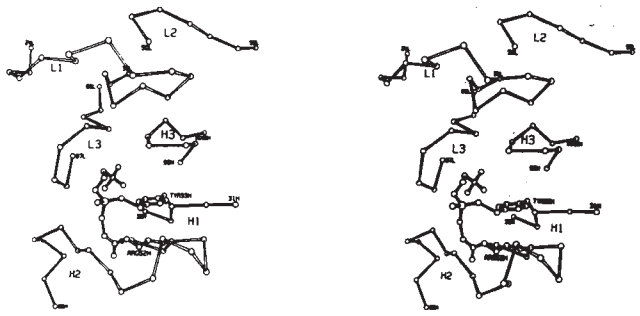

FIG. 3. Stereo drawing of the hypervariable cavity with phosphorylcholine bound. The six hypervariable loops are shown together with the side chains of Tyr 33(H) and Arg 52(H). Note the position of L2 which is screened from interaction with the hapten by the extended L1 loop. The orientation is approximately the same as in Fig. 4 of Amzel *et al.* (8).

of residues 102–103 of the H chain and residues 91–94 of the L chain. The entire hapten is in close van der Waals contact with the ring atoms of Tyr 33(H).

DISCUSSION

The close similarity between this mouse 603 IgA(K) Fab and the human New IgG(λ) Fab (7) in both their tertiary and quaternary structures, coupled with the similar structures observed for human Bence-Jones dimers (9, 10), strongly implies the invariance of many structural features in the architecture of antibodies. However, the considerable differences in the overall shape, size, and general chemical nature of the antigen-binding sites provides a plausible and sufficient structural explanation for antibody diversity.

A comparison of the two variable domains of McPC 603 shows them also to be very similar except in the hypervariable regions. When one domain is fitted to the other by a least squares procedure, the root-mean-square distance between the alpha carbon atoms of 74 homologous residues is 1.9 Å.

It is interesting that a similar comparison of V_L (603) with V_L(REI) (10) shows that they resemble each other even more closely, with a root-mean-square distance of 1.4 Å between 94 homologous residues in the nonhypervariable regions. This is very close agreement in view of the fact that the 603 coordinates have not yet been refined. A detailed comparison is not yet possible with the human Fab (7) and the Bence-Jones dimer (9), and will have to await further data.

Such comparisons are meaningless when applied to the hypervariable regions, because of the numerous insertions and deletions that occur in these portions of the molecule. It is nevertheless clear that the folding of these regions varies greatly from one molecule to the next. Sequence comparisons of the light and heavy chains of 603 with other immunoglobulins reveal a six-residue insertion in L1. This results in a large convoluted loop which provides a larger surface for interaction with antigen while at the same time masking the potential involvement of L2 in binding with hapten.

In the heavy chain, by contrast, H1 is of normal length, while H2 has a two-residue insertion. These two residues are in addition to the five by which the heavy chain is usually greater than the light in this region (19). The effect of these extra residues is to make H2 extend much farther out, providing a much bigger surface for interaction with antigen. The H3 region also has a two-residue insertion.

There are two consequences of these insertions in McPC 603. The first is to provide an extensive hypervariable surface with a large cavity. The second consequence of these insertions is to make the cavity quite asymmetric, making the antigen-binding site of McPC 603 quite different from the symmetric hypervariable cavities of the two human Bence-Jones dimers (9, 10). By contrast, the site of hydroxy vitamin K_1 binding in Fab New is relatively flat, with a shallow groove between the two domains (8).

The hapten binding in the McPC 603 is predominantly with the heavy chain. This observation is consistent with affinity labeling studies (21), which demonstrated an 8:1 preference for H chain labeling. In contrast, the methylnaphthoquinone ring of hydroxyvitamin K_1 interacts principally with L1, L2, and H3 of the Fab New with only the end of the phytyl chain interacting with H1 and H2. In addition to this difference in the location of the binding site, there are also differences in the nature of the protein–ligand interactions. At pH 7, phosphorylcholine can be expected to have two negative charges on the phosphate and one positive charge on the quaternary nitrogen of the choline. It is not surprising, therefore, that strong interactions occur between this hapten and charged groups such as Arg 52(H), Lys 54(H), and Glu 35(H). The electronegative oxygens of the phosphate groups form strong hydrogen bonds with the phenolic hydroxyl of Tyr 33(H) and with an amino group of Arg 52(H). Hydroxyvitamin K_1 on the other hand, cannot be expected to participate in electrostatic interactions with charged groups, and it is not entirely surprising that the aromatic methylnaphthoquinone moiety forms a close contact with the ring of Tyr 90(L) (8). It should be noted that despite the disparity in size between hydroxyvitamin K_1 and phosphorylcholine, they both bind to their respective proteins with roughly equal affinity (8, 1).

These studies demonstrate the involvement of many amino acids from the hypervariable loops of the two chains in hapten binding, in spectacular confirmation of the hypothesis of Wu and Kabat (16). In the case of McPC 603, in particular, the binding studies illustrate the stringent requirements for complementarity for the hapten–protein interactions. Changes in specificity might be produced in at least three different ways. First, there are simple substitutions of amino acids; in the case of McPC 603, for example, a substitution of glutamic acid for Arg 52(H) would probably not affect the overall topology of the binding surface, but should dramatically change its binding properties. Second, there are insertions and deletions within the hypervariable regions. They can profoundly alter the folding of the hypervariable loops, thus producing an effect that is greater than that due to merely substituting additional amino-acid side chains into the cavity. Insertions and deletions can also alter the shape and extent of the hypervariable cavity. Finally, there is the possibility that either by amino-acid substitutions or by insertions or deletions one may alter the interactions between the two variable domains, resulting in a change in their relative positions or orientations. Thus, by altering the relative positions of the light and heavy chain hypervariable loops, significant changes in specificity can be produced. While present data do not permit a test of this possibility to be made, further comparative studies [e.g., with J539, a mouse IgA(K) Fab with galactan specificity] should reveal its importance as a mechanism of antibody variability.

Phosphorylcholine, being a small molecule, interacts with relatively few amino acids at the binding site. It is interesting

to speculate what might be the function of the remainder of hypervariable surface of the molecule.

The most likely explanation is that the true antigenic determinant is much larger than phosphorylcholine and would probably fill most of the site.

Another possible use of the remaining portion of the McPC 603 hypervariable surface would be to bind a completely unrelated, and as yet undefined, antigen. In this regard, either phosphorylcholine or any other hypothetical unrelated substance would be considered an antigen for McPC 603 if it elicited antibody production. Indeed, antibody populations typically contain members capable of crossreacting and being elicited by unrelated antigens (22). Of course, the remainder of the potential binding site may not recognize any foreign substance and merely be, in this case, vestigial.

The location of the phosphorylcholine binding site, surrounded as it is by the high walls containing hypervariable residues, provides a simple structural basis for the existence of two classes of hypervariable region related idiotypic determinants: those which act independently of hapten binding (e.g., L2 in 603) and those which are correlated with hapten binding. Other non-hypervariable areas in the variable domain could also provide sources of idiotypic determinants.

The results of the 4.5-Å study on phosphorylcholine binding to McPC 603 (2), supported by the hydroxyvitamin K_1 binding studies on Fab New (8), show very clearly that binding is unaccompanied by a major conformational change in the Fab fragment in the crystal. This result implies that hapten binding in solution will leave the overall configuration of the fragment unchanged in agreement with low-angle x-ray scattering observations (23). It thus seems likely that the structural basis of antibody effector reactions, such as complement fixation or B cell activation, must occur through a mechanism not involving a major rearrangement of the Fab conformation.

It is interesting to note that although the tertiary structures of the variable and constant domains are very similar, their interaction in pairs is very different. The interface between variable domains involves one surface of the domain bilayer sandwich, while the constant domain interface involves the other side. The relatively strong homology between C_L, C_H1, C_H2, and C_H3 domains (24) leads us to conclude that the quaternary structure of the C_H2 and C_H3 regions of the Fc part of the molecule will closely resemble the structure observed here for the constant region of the Fab.

We thank Dr. Matthew D. Scharff for preserving the McPC 603 cell line, and Dr. Enid Silverton for allowing us to quote results prior to publication.

1. Rudikoff, S., Potter, M., Segal, D. M., Padlan, E. A. & Davies, D. R. (1972) *Proc. Nat. Acad. Sci. USA* **69**, 3689–3692.
2. Padlan, E. A., Segal, D. M., Spande, T., Davies, D. R., Rudikoff, S. & Potter, M. (1973) *Nature New Biol.* **245**, 165–167.
3. Potter, M. (1972) *Physiol. Rev.* **52**, 631–719.
4. Potter, M. (1971) *Ann. N.Y. Acad. Sci.* **190**, 306–321.
5. Blomberg, B., Carlson, D. & Weigert, M. (1972) in *3rd Int. Convocation Immunology, Buffalo, N.Y.* (Karger, Basel, 1973), pp. 285–293.
6. Lieberman, R., Potter, M., Mushinski, E. B., Humphrey, W., Jr. & Rudikoff, S. (1974) *J. Exp. Med.* **139**, 983–1001.
7. Poljak, R. J., Amzel, L. M., Avey, H. P., Chen, B. L., Phizackerly, R. P. & Saul, F. (1973) *Proc. Nat. Acad. Sci. USA* **70**, 3305–3310.
8. Amzel, L. M., Poljak, R. J., Saul, F., Varga, J. M. & Richards, F. F. (1974) *Proc. Nat. Acad. Sci. USA* **71**, 1427–1430.
9. Schiffer, M., Girling, R. L., Ely, K. R. & Edmundson, A. B. (1973) *Biochemistry* **12**, 4620–4631.
10. Epp, O., Colman, P., Fehlhammer, H., Bode, W., Schiffer, M., Huber, R. & Palm, W. (1974) *Eur. J. Biochem.* **45**, 513–524.
11. Richards, F. M. (1968) *J. Mol. Biol.* **37**, 225–230.
12. Diamond, R. (1966) *Acta Crystallogr.* **21**, 253–266.
13. Francis, S. H., Leslie, G. Q., Hood, L. & Eisen, H. N. (1974) *Proc. Nat. Acad. Sci. USA* **71**, 1123–1127.
14. Svasti, J. & Milstein, C. (1972) *Biochem. J.* **128**, 427–444.
15. Gray, W. R., Dreyer, W. J. & Hood, L. (1967) *Science* **155**, 465–467.
16. Wu, T. T. & Kabat, E. A. (1970) *J. Exp. Med.* **132**, 211–250.
17. Rudikoff, S. & Potter, M. (1974) *Biochemistry* **13**, 4033–4038.
18. Venkatachalam, C. M. (1968) *Biopolymers* **6**, 1425–1436.
19. Dayhoff, M. O., Ed. (1972) *Atlas of Protein Sequence and Structure* (National Biomedical Research Foundation, Washington, D.C.).
20. Capra, J. D. & Kehoe, J. M. (1974) *Proc. Nat. Acad. Sci. USA* **71**, 845–848.
21. Cheesebro, B., Hadler, N. & Metzger, H. (1972) in *3rd Int. Convocation Immunology, Buffalo, N.Y.* (Karger, Basel, 1973), pp. 205–217.
22. Rosenstein, R. W., Musson, R. A., Armstrong, M. Y. K., Konigsberg, W. H. & Richards, F. F. (1972) *Proc. Nat. Acad. Sci. USA* **69**, 877–881.
23. Pilz, I., Kratky, O. & Karush, F. (1974) *Eur. J. Biochem.* **41**, 91–96.
24. Edelman, G. M., Cunningham, B. A., Gall, W. E., Gottlieb, P. D., Rutishauser, U. & Waxdal, M. J. (1969) *Proc. Nat. Acad. Sci. USA* **63**, 78–85.
25. Barstad, P., Rudikoff, S., Potter, M., Cohn, M., Konigsberg, W. & Hood, L. (1974) *Science* **183**, 962–964.